New All-Aromatic Liquid Crystal Architectures

Nicholas A. Zafiropoulos,[†] E-Joon Choi,[‡] Theo Dingemans,[§] Wenbin Lin,[†] and Edward T. Samulski*,[†]

Department of Chemistry, University of North Carolina at Chapel Hill, Chapel Hill, North Carolina 27599-3290, Department of Polymer Science and Engineering, Kumoh National Institute of Technology, Kumi, Kyungbuk 730-701, Korea, and Faculty of Aerospace Engineering, Delft University of Technology, Kluyverweg 1, 2629 HS, Delft, The Netherlands

Received July 16, 2007. Revised Manuscript Received March 21, 2008

We have explored oxadiazole and thiophene modifications of the classic calamitic mesogens, *p*-quinquephenyl, *p*-sexiphenyl, and *p*-septiphenyl (P_n, $n = 5$, 6, and 7). Replacing a phenyl ring with 2,5-substituted 1,3,4-oxadiazole and 2,5-substituted thiophene introduces a bend, or kink, into the parent mesogens of 134 and 148°, respectively. When oxadiazole was placed at penultimate positions on both ends of the mesogen (P**O**P_n**O**P, $n = 1$, 2, and 3), a significant reduction in melt transitions for all model compounds could be observed. *p*-Septiphenyl (P_7) is an intractable and infusible molecule but its oxadiazole analogue P**O**P_3**O**P melts at 312 °C, exhibiting a broad nematic range 170° wide. Replacing the central para-substituted phenylene ring in P**O**P_3**O**P with an ortho- or a meta-substituted phenylene, however, destroys the LC behavior completely; the ortho-derivative forms an amorphous glass ($T_g = 83$ °C). Comparisons of the P_6 derivatives with the oxadiazoles in P**O**PP**O**P replaced with 2,4- and 2,5-substituted thiophenes show that the LC phase is completely lost for the 2,4-thiophene derivative (2,4-P**T**PP**T**P). The more linear 2,5-thiophene isomer (2,5-P**T**PP**T**P), with an exocyclic bond angle $\epsilon = 148°$, shows a broad LC range with both nematic and SmA phases. This suggests that in addition to mesogen shape, electronic conjugation and electrostatic considerations are important mesophase stabilizing factors in this class of all-aromatic liquid crystals. A 1,3,5-tris(oxadiazole) discoid, i.e., P(**O**P)$_3$, was synthesized but no mesophase behavior could be detected; this absence of mesogenicity was consonant with the X-ray determined packing motif for P(**O**P)$_3$.

Introduction

Statistically linear liquid crystal molecules (calamitic mesogens) account for the bulk of nematics, fluids that exhibit long-range, uniaxial, molecular orientational order. This order gives rise to anisotropic properties of the fluid (refractivity, permittivity, etc.), which in turn enables the electro-optic switching phenomena underpinning liquid crystal displays (LCDs). The advent of unconventional liquid crystal molecular architectures over the last three decades, such as disk-shaped molecules (discotic mesogens)[1] and nonlinear molecules (bent-core or banana mesogens),[2] has started to reveal unique insights into how mesogen shape manifests itself in the symmetry of the supramolecular organization in columnar and stratified smectic liquid crystal (LC) phases, respectively. For example, achiral, nonlinear banana mesogens may exhibit smectic phases displaying supramolecular ferro- and antiferroelectricity,[3] chirality,[4] and biaxiality.[5] In calamitic, discotic, and banana LCs, flexible aliphatic chains appended to the periphery of the shape-dictating mesogenic core play an important but still ill-defined role: thermally induced disorder among these flexible appendages at the crystal-to-fluid phase transition entropically stabilizes delicate supramolecular structures that in the case of nematics, have no long-range translational order. Generally, flexible chains lower transition temperatures thereby increasing the thermal range of the LC phases. Also, above a critical chain length, this high-entropy component of mesogens nanophase separates into strata thereby promoting smectic mesophase formation. However, molecular flexibility—both conformational changes within the core and chain isomerization—blurs the role of mesogen shape in determining liquid crystal phase type; flexible molecules can readily acquiesce to external intermolecular packing constraints hence it becomes difficult to understand if molecular shape plays a dominant role in the ultimate supramolecular organization within these unusual fluid phases, or if molecular (statistical) shape is a consequence of the constraints flexible mesogens experience in the LC's anisotropic mean field.

We have explored how mesogen shape and mesogen electrostatic profile impact phase type and stability in mesogens devoid of flexible components, i.e., molecules with

* To whom correspondence should be addressed. Phone: (919) 962-1561. Fax: (919) 962-7267. E-mail: et@unc.edu.
[†] University of North Carolina at Chapel Hill.
[‡] Kumoh National Institute of Technology.
[§] Delft University of Technology.

(1) Chandrasekhar, S.; Ranganath, G. S. *Rep. Prog. Phys.* **1990**, *53*, 57.
(2) Pelzl, G.; Diele, S.; Weissflog, W. *Adv. Mater.* **1999**, *11*, 707.
(3) Walba, D. M.; Kšrblova, E.; Shao, R.; Maclennan, J. E.; Link, D. R.; Glaser, M. A.; Clark, N. A. *Science* **2000**, *288*, 2181.
(4) Link, D. R.; Natale, G.; Shao, R.; Maclennan, J. E.; Clark, N. A.; Kšrblova, E.; Walba, D. M. *Science* **1997**, *278*, 1924.
(5) Madsen, L. A.; Dingemans, T. J.; Nakata, M.; Samulski, E. T. *Phys. Rev. Lett.* **2004**, *92* (145505), 1–4.

10.1021/cm701862w CCC: $40.75
Published on Web 05/27/2008

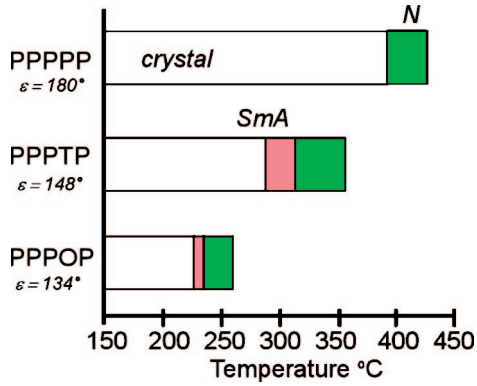

Figure 1. Mesophase behavior of thiophene (T) and oxadiazole (O) modifications of *p*-quinquephenyl (PPPPP).[6] Both a smectic-A (SmA) and a nematic (N) phase are observed when T (exocyclic bond angle $\epsilon = 148°$) and O ($\epsilon = 134°$) are substituted into the "2" position of the parent PPPPP.

minimal internal degrees of freedom within the core, and without pendant flexible aliphatic chains. To that end, we recently reported that such nonlinear mesogens could be prepared by introducing five-membered heterocyclic rings into a linear, conjugated aromatic mesogen architecture. For example, we introduced 2,5-substituted thiophene, 1,3,4-oxadiazole, and oxazole (exocyclic bond angles $\epsilon = 148$, 134, and 132°, respectively) into the linear *p*-quinquephenyl (I, $n = 5$) parent mesogen abbreviated PPPPP.[6]

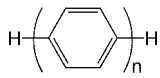

(**I**)

The general features of our findings are summarized in Figure 1. For example, translating 2,5-thiophene from the terminal "1" position (PPPP**T**) to the "2" position (PPP**T**P) resulted in reduction of the N−I transition by 64°. The reduction is much larger in the more acute shaped PPP**O**P (∼160°). In addition, we observed the formation of nematic (N) and smectic A (SmA) phases in both derivatives with a significant increase in the mesophase range for PPP**T**P (67° versus a 32° range for PPPPP). From these observations, we concluded that steric (excluded volume) packing considerations dominate the phase type preferences, i.e., nematic versus smectic phases, and that electronic conjugation appeared to control the phase thermal stability range in this family of all-aromatic liquid crystals. Here we pursue extensions of all-aromatic mesogen architectures by synthesizing several new liquid crystal shapes ranging from linear calamitic to nonlinear and discotic mesogens by appropriate modifications of *p*-quinquephenyl (I, $n = 5$), *p*-sexiphenyl (I, $n = 6$), and *p*-septiphenyl (I, $n = 7$).[7–10]

(6) Dingemans, T. J.; Murthy, N. S.; Samulski, E. T. *J. Phys. Chem. B* **2001**, *105*, 8845.
(7) Irvine, P. A.; Wu, D. C.; Flory, P. J. *J. Chem. Soc., Faraday Trans. 1* **1984**, *80*, 1795.
(8) Flory, P. J.; Irvine, P.; A, *J. Chem. Soc., Faraday Trans. 1* **1984**, *80*, 1807.
(9) Irvine, P. A.; Flory, P. J. *J. Chem. Soc., Faraday Trans. 1* **1984**, *80*, 1821.
(10) Flory, P. A.; Ronca, G. *Mol. Cryst. Liq. Cryst.* **1979**, *54*, 311.

Target Mesogen Architectures

POP$_n$OP. In the first target series, *p*-quinquephenyl, *p*-sexiphenyl, and *p*-septiphenyl were modified by placing oxadiazole at the "2" positions, i.e., the penultimate phenyl rings were replaced with a 2,5-connected heterocycle. By doing so, the linearity at both ends of the parent mesogen is interrupted, and in the resulting P**O**P$_n$**O**P molecules, a strong local electrostatic dipole moment (∼ 4 D) bisecting the heterocycle is introduced near the termini of the molecules.[11]

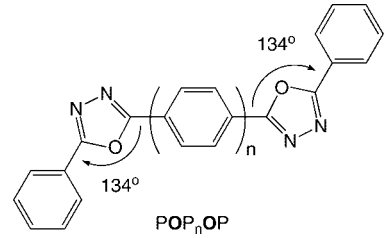

POP$_n$OP

We also studied analogues of P**O**P$_n$**O**P with $n = 2$ in the form of the 2,5-substituted thiophene (2,5-P**T**PP**T**P) and 2,4-substituted thiophene (2,4-P**T**PP**T**P).

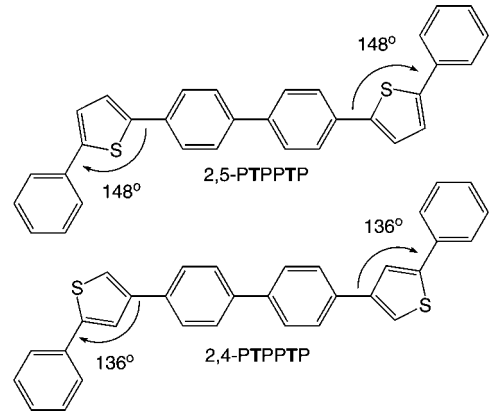

POPP′POP. To probe core nonlinearity within the class of P**O**P$_n$**O**P mesogens, we targeted 1,3- and 1,2-phenylene isomers, *o*-P**O**PP′P**O**P and *m*-P**O**PP′P**O**P, wherein the substitution pattern of the central phenylene (P′) was changed. These substitutions introduce 60 and 120° bends into the mesogenic cores, respectively.

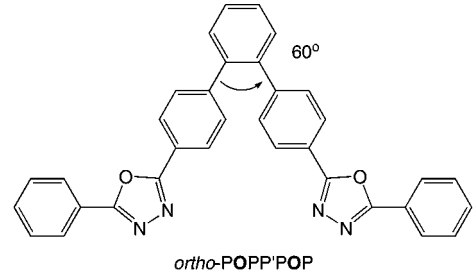

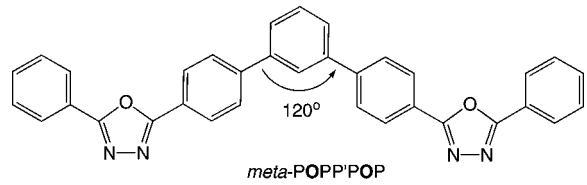

Scheme 1. Synthesis of Oxadiazole-Modified *p*-Phenylene Model Compounds

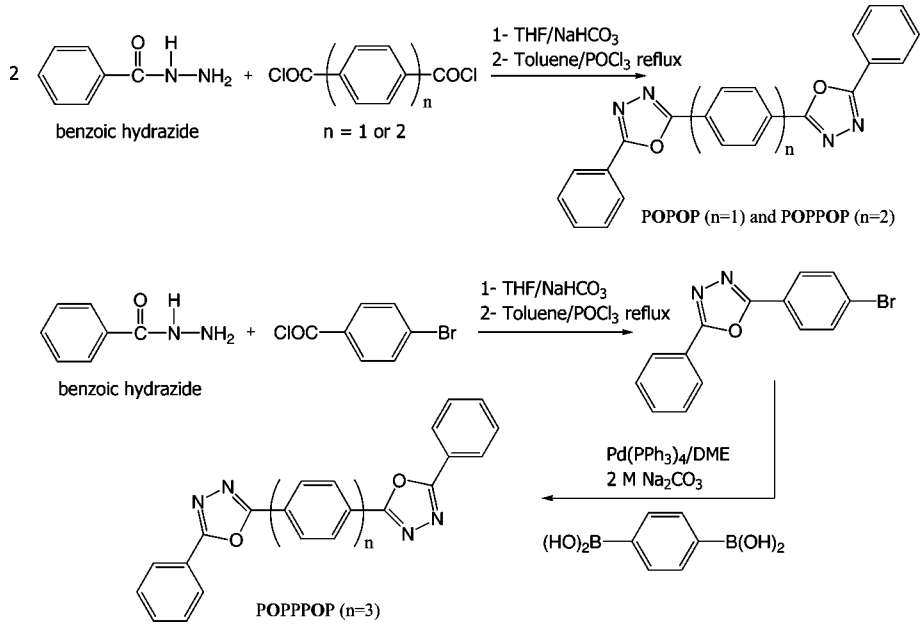

P(OP)$_3$. Lastly, trimeric disk- or star-shaped architectures were examined by exploiting a trisubstituted central aromatic ring:

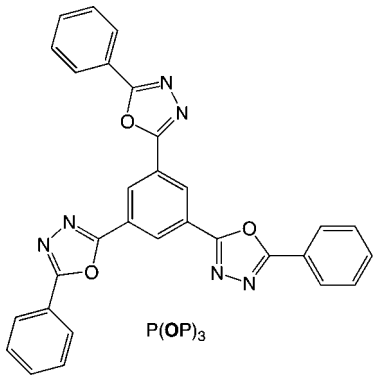

Synthetic Strategy

Where appropriate, we employed the Suzuki cross-coupling strategy to form multiaryl heterocyclic systems. This technique allowed usage of commercially available aryl boronic acids and the appropriate aryl bromides in the presence of Pd(0) catalyst and base.[6,12] The yields are usually high and side reactions are limited. The 2,5-substituted 1,3,4-oxadiazole intermediates were synthesized by coupling the appropriate benzoic hydrazide and acid chloride under basic conditions, followed by dehydration to afford the desired closed ring structure.[13] 2,4- and 2,5-Thiophene heterocyclic intermediates were made according to procedures earlier described by us.[6]

Scheme 1 shows the synthesis of the first series of oxadiazole modified *p*-phenylene model compounds, i.e., P**O**P$_n$**O**P, where n = 1, 2, or 3. The 5- and 6-ring systems, i.e.. *p*-P**O**P**O**P and *p*-P**O**PP**O**P, were synthesized via the classic route as described by Wang et al.[13] Terephthaloyl- and 4,4′-biphenyldicarbonyl chloride were coupled with benzoic hydrazide, and the resulting hydrazides were then dehydrated in refluxing $POCl_3$ and toluene. The 7-ring system, i.e., *p*-P**O**PPP**O**P, was synthesized by coupling 2-(4-bromophenyl)-5-phenyl-1,3,4-oxadiazole with 1,4-phenylenebisboronic acid under Suzuki cross-coupling conditions. The synthesis of 2-(4-bromophenyl)-5-phenyl-1,3,4-oxadiazole was reported by us previously.[6] In a similar fashion, *m*-P**O**P**O**P was made as described for *p*-P**O**P**O**P, starting from isophthaloyl chloride.

Meta and ortho derivatives of P**O**PPP**O**P were both synthesized from their respective *m*- and *o*-terphenyl cores. The synthesis of *o*-P**O**PPP**O**P is shown in Scheme 2 below. The key intermediate, 4,4′-*o*-terphenyldicarboxylic acid, was prepared by dicarboxylation with oxalyl chloride under Friedel−Crafts conditions. Treatment with thionyl chloride afforded 4,4′-*o*-terphenyldicarbonyl chloride, which was coupled with benzoic hydrazide and dehydrated to yield the desired *o*-P**O**PPP**O**P compound. *m*-P**O**PPP**O**P was made in a similar fashion.

Intermediates for the syntheses of 2,5-P**T**PP**T**P and 2,4-P**T**PP**T**P, 2-phenyl-5-thiopheneboronic acid and 4-phenyl-2-thiopheneboronic acid, respectively, were reported in a previous paper.[6] Under Suzuki cross-coupling conditions, bis-substitution to 4,4′-dibromobiphenyl gave the desired mesogenic systems, as summarized in Scheme 3.

We also investigated the possibility of forming star-shaped, or discotic, liquid crystals based on substituted tris-1,3,4-oxadiazoles. Scheme 4 shows the synthesis of a star-shaped model compound.

Results

Before we present the new results, we recall the behavior of the parent para-linked oligophenylenes: The first member

(11) Clapp, L. B. 1,2,4-Oxadiazoles. In *Advances in Heterocyclic Chemistry*; Katritzky, A. R.; Boulton, A. J., Eds.; Academic Press: New York, 1974; Vol. 20.
(12) Hird, M.; Gray, G. W.; Toyne, K. J. *Mol. Cryst. Liq. Cryst.* **1991**, *206*, 187.
(13) Wang, R. H. S.; Irick, G. U.S. Patent 4,043,973, 1977.

Scheme 2. Synthesis of the *o*-POPPPOP Model Compound

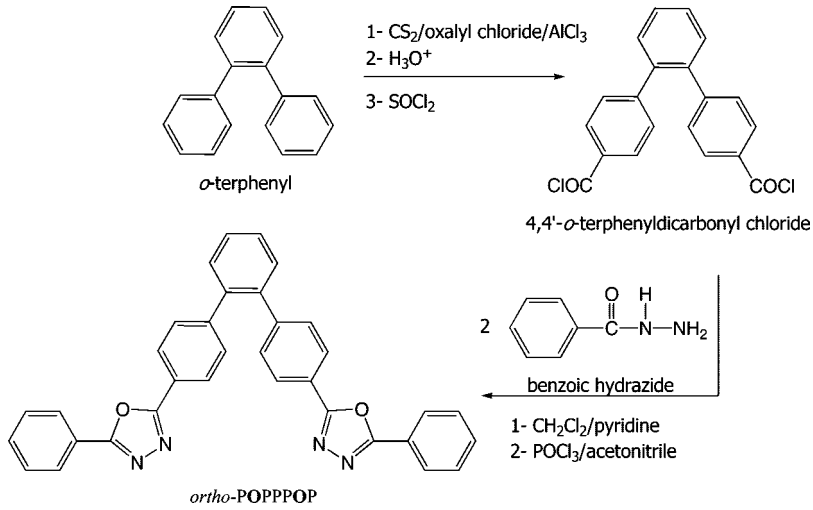

Scheme 3. Synthesis of 2,5-PTPPTP and 2,4-PTPPTP Mesogens with Exocyclic Bond Angles ϵ =148 and 136°, Respectively

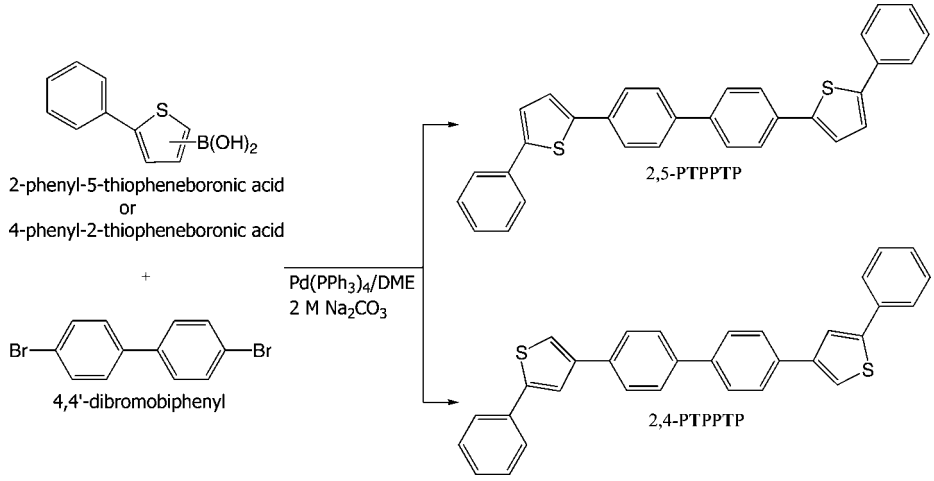

of the all-aromatic homologous series, *p*-quinquephenyl (I, $n = 5$), is the only mesogen that forms a thermally stable nematic melt (388−420 °C).[6–10] The next member, *p*-sexiphenyl, is extremely high melting (440 °C)[7–10] and can be studied only using fast heat and cooling rates of 50 and 25 °C min^{-1}, respectively, to prevent thermal degradation. The last compound, *p*-septiphenyl, does not melt at all and is completely intractable. Very different behavior is observed when we interject 2,5-substituted 1,3,4-oxadiazole (**O**) and 1,4-, 1,3-, or 1,2-phenylene (P) units into the oligophenylene framework.

Thermal Analysis. The DSC results of a series of the mesogens *p*-POPOP, *p*-POPPOP and *p*-POPPPOP derived from the parent *p*-phenylenes (I) with $n = 5$, 6, and 7 are presented in Table 1. All transition temperatures are lowered when nonlinearity, in the form of a 2,5-disubstituted-1,3,4-oxadiazole moiety (exocyclic bond angle $\epsilon \approx 134°$), is introduced into the linear *p*-phenylene parent mesogen. The first member of this series, i.e., *p*-POPOP, melts at 302 °C, which is a reduction of ∼80 °C relative to the parent compound *p*-quinquephenyl (PPPPP) ($T_{Cr-I} = 388$ °C).[6] The compromised molecular shape—no extended shape anisotropy and partial disruption of the conjugation by the heterocycles—prevents the formation of a stable mesophase. However, as the number of central phenylene units increases, we observe broad nematic ranges ($\Delta T_N = T_{I-N} - T_{N-Cr}$) for both *p*-POPPOP ($\Delta T_N = 59°$) and *p*-POPPPOP ($\Delta T_N = 170°$).

From these results, it is evident that introducing "kinked" moieties in the parent *p*-oligophenylenes suppresses the melting point but does not inhibit the formation of nematic LC phases. Both parent LCs are extremely high melting, i.e., sexiphenyl (**I**, $n = 6$), or decompose before they melt, as is the case for septiphenyl (**I**, $n = 7$), making the *p*-oligophenylenes very difficult to investigate. Introducing two nonlinear oxadiazole moieties, however, suppressed the formation of the smectic phase that *p*-sexiphenyl displays, and when we modified only one end of *p*-quinquephenyl (PPPPP) with an oxadiazole unit at the "2"-position PPPOP, this mesogen also exhibited a SmA phase.[6]

Encouraged by the observation that *p*-POPPPOP displays a nematic liquid crystalline phase over a very wide temperature range ($\Delta T_N = 170°$), we used this mesogen as a starting point for investigating the effects of constructing more extreme molecular architectures with an aim of understanding the role of nonlinear geometries on mesophase formation. Table 2 shows the DSC results of our seven-ring systems where we contrast the *o*-POPP′POP and *m*-POPP′POP thermal transitions with that of *p*-POPPPOP. The change in overall molecular shape is unambiguous varying from 180° (para) to 120° (meta) and to 60° (ortho) as the substitution

Scheme 4. Synthetic Route to 1,3,5-Tris(5-phenyl-1,3,4-oxadiazole-2-yl)benzene, P(OP)$_3$

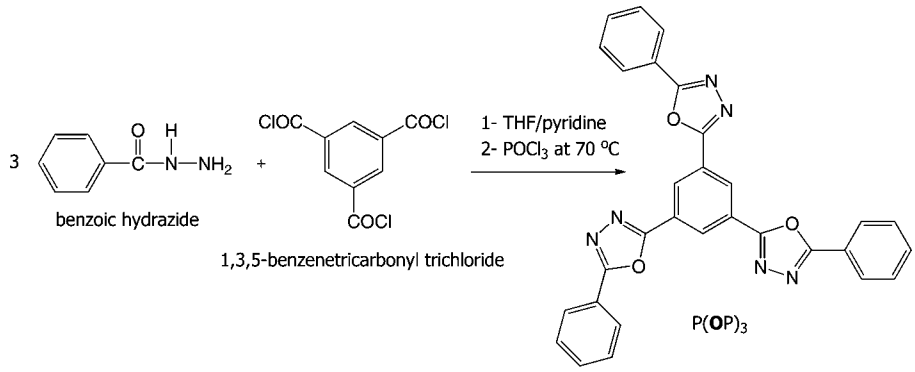

Table 1. Transition Temperatures (°C) and Enthalpies (kJ mol^{-1}; in italics) for Second Heating and Cooling (10° min^{-1}) of the POP$_n$OP Compounds

NAME	STRUCTURE	PHASE MAP (^{o}C/*kJ mol^{-1}*)
p-POPOP	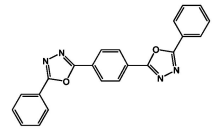	Cr ⇄ I: 302(*5*) / 289(*-4*)
p-POPPOP	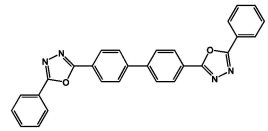	Cr ⇄ N ⇄ I: 269(*9*) / 253(*-7*); 312(–)^{a} / 312(–)^{a}
p-POPPPOP	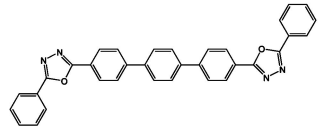	Cr → Cr' ⇄ N ⇄ I: 259(*2*); 312(*9*) / 274(*-9*); 444(–)^{b} / 444(–)^{b}

^{a} T_{N-I} could be observed only using optical microscopy. ^{b} T_{N-I} and associated enthalpy could not be determined because of thermal decomposition.

pattern on the central phenyl is altered. The nonlinear *m*-POPP′POP exhibits a single crystalline to isotropic transition at 274 °C on heating and two crystal−crystal transitions (Cr−Cr′ and Cr′−Cr″) upon cooling, however no mesophase behavior could be observed. A lack of mesophase behavior was also observed for the more acute nonlinear *o*-POPP′POP. In addition, for *o*-POPP′POP, we detected crystal melting on the first heat only. Consecutive heating and cooling experiments, using different cooling rates, yielded an amorphous glass with a glass-transition temperature of $T_g \approx 73$ °C. Similar to *o*-terphenyl itself, the significant deviation of the molecular framework of *o*-POPP′POP from linearity probably accounts for its propensity to form a glass on cooling from its melt.

To probe the role of the heterocycle's exocylic bond angle (ϵ) on the mesophase behavior of these all-aromatic LCs, we synthesized two heterocylic modifications of *p*-POPPOP wherein the oxadiazole moiety was replaced with 2,5-substituted thiophene, 2,5-PTPPTP, or 2,4-substituted thiophene, 2,4-PTPPTP. The DSC results for this series of molecules are summarized in Table 3 below.

It was evident from the DSC results that the nature of the heterocycle and its substitution pattern—the ability of the heterocyle to propagate electronic conjugation to neighboring phenyl rings—has a dramatic effect on the melting point, the phase range and the phase type. Both *p*-POPPOP and 2,4-PTPPTP have very similar molecular geometries, i.e., 2,5-substited oxadiazole and 2,4-substituted thiophene each have a $\epsilon \approx 136°$ exocyclic bond angle and consequently produce identical kinks at the termini of each molecule. However, *p*-POPPOP shows a stable enantiotropic liquid crystal with $\Delta T_N = 59°$, but 2,4-PTPPTP does not show any mesomorphism. When thiophene is "rotated" to its 2,5-substitution pattern ($\epsilon = 148°$), as is the case for 2,5-PTPPTP, both a SmA and a N phase were observed and the liquid crystal phases persists over a 97° temperature window. To the best of our knowledge, this is only the third example of a wholly aromatic liquid crystal that forms a SmA phase; *p*-sexiphenyl (PPPPPP)[7–10] and 2-terphenyl-4-*yl*-5-phenyl thiophene (PPPTP)[6] are the other two examples reported to date.

The symmetric structure of 2,5-PTPPTP exhibits a mesophase range similar to its parent *p*-sexiphenyl although

Table 2. Transition Temperatures (°C) and Enthalpies (kJ mol^{-1}; in italics) for Second Heating and Cooling (10° min^{-1}) of the Oxadiazole-Containing Isomers of POPPPOP

NAME	STRUCTURE	PHASE MAP (°C/*kJ mol^{-1}*)
p-POPPPOP	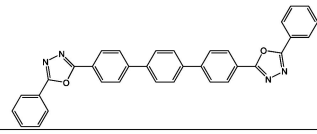	Cr $\xrightarrow{259(2)}$ Cr' $\underset{274(-9)}{\overset{312(9)}{\rightleftharpoons}}$ N $\underset{444(-)^a}{\overset{444(-)^a}{\rightleftharpoons}}$ I
m-POPP'POP	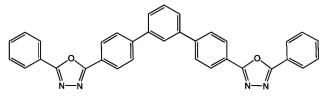	Cr'' $\underset{201(-0.1)}{\overset{}{\leftarrow}}$ Cr' $\underset{209(-0.3)}{\overset{}{\leftarrow}}$ Cr $\underset{231(-14)}{\overset{274(15)}{\rightleftharpoons}}$ I
o-POPP'POP	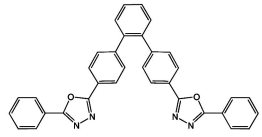	Cr $\xrightarrow{197(32)}$ I g $\xleftarrow[83]{}$ I

[a] T_{N-I} and associated enthalpy could not be determined because of thermal decomposition.

Table 3. Transition Temperatures (°C) and Enthalpies (kJ mol^{-1}; in italics) for Second Heating and Cooling (10° min^{-1}) of the Thiophene- and Oxadiazole-Containing Six-Ring Compounds

NAME	STRUCTURE	PHASE MAP (°C/*kJ mol^{-1}*)
p-POPPOP (ε=136°)	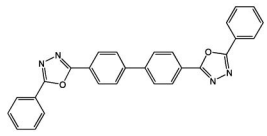	Cr $\underset{253(-7)}{\overset{269(9)}{\rightleftharpoons}}$ N $\underset{312(-)^a}{\overset{312(-)^a}{\rightleftharpoons}}$ I
2,4-PTPPTP (ε=136°)	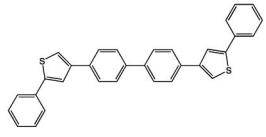	Cr $\underset{323(-16)}{\overset{341(17)}{\rightleftharpoons}}$ I
2,5-PTPPTP (ε=148°)	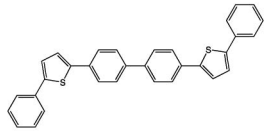	Cr $\underset{345(-5)}{\overset{358(12)}{\rightleftharpoons}}$ SmA $\underset{366(-0.1)}{\overset{367(0.2)}{\rightleftharpoons}}$ N $\underset{455(-0.1)}{\overset{455(0.1)}{\rightleftharpoons}}$ I

[a] T_{N-I} could be observed only using optical microscopy.

nearly 100° lower in temperature. The differences in phase behavior between *p*-POPPOP ($\epsilon = 134°$) and 2,4-PTPPTP ($\epsilon = 136°$) could be attributed to several factors: In our previous work, we have shown that geometrical isomers of the 2,5-substituted thiophene-based liquid crystal, PPPTP, where the thiophene moiety was "rotated" to yield 3,5- and 2,4- substitution patterns, exhibited monotropic nematic phases stable over a one- or two-degree temperature range.[6] This effect was attributed to the interruption of conjugation in the 3,5- and 2,4-isomers, which in turn produces lower values of the electronic polarizability and thereby reduces the anisotropy of the attractive interactions relative to those operative in 2,5-substituted PPPTP. In addition, strong dipole−dipole interactions between the *p*-POPPOP mesogens − the electrostatic dipole moment of 2,5-diphenyl-1,3,4-oxadiazole is ~4.0 D[11]− could provide additional mesophase stabilization. Similar arguments, we believe, might underlie the observation of only a Cr-to-I transition for 2,4-PTPPTP.

In the final series, we attempted to explore the possibility of columnar mesomorphism in this class of materials by synthesizing disk-shaped molecules based on the POP theme. The DSC results for these new materials are summarized in Table 4.

Table 4. Transition Temperatures (°C) and Enthalpies (kJ mol^{-1}; in italics) for the Second heating and Cooling (10° min^{-1}) of *m*-POPOP and P(OP)$_3$[a]

NAME	STRUCTURE	PHASE MAP (°C/*kJ mol^{-1}*)
m-POPOP	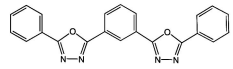	Cr ⟵ 208(*-0.1*) Cr' ⟶ 245(*10*) ⟵ 225(*-10*) I
P(OP)$_3$	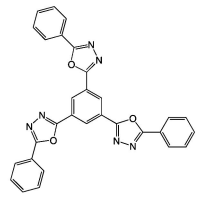	Cr ⟶ 337(*15*) ⟵ 321(*-14*) I

[a] The slightest amount of impurity suppresses the melting point of P(OP)$_3$ and results in the formation of a nematic texture, as observed by optical microscopy.

Figure 2. Microphotographs (crossed polars; 20×) of the liquid crystalline phases of 2,5-PTPPTP: (left) focal-conic texture of the smectic-A phase (360 °C); (right) threaded nematic phase (440 °C).

Optical Microscopy. The phase behavior of all model compounds was investigated using hot-stage polarizing optical microscopy. All samples were studied between untreated glass slides using heating and cooling rates of 10° min^{-1}. Despite the relatively high transition temperatures, all liquid crystals form stable mesophases under atmospheric conditions. The only exception is *p*-POPPPOP, which decomposes at temperatures above 400 °C, as became evident by strong colorization of the sample. All liquid crystals form low viscosity nematic melts with a strong tendency to form homeotropic textures.

In Figure 2, we show the two liquid crystal textures of 2,5-PTPPTP. Upon cooling from the isotropic phase a nematic "threaded" texture was observed at 440 °C. This texture is representative for all LCs, i.e., no 2- or 4-brush disclinations could be recognized. When cooling was continued, the nematic phase transformed into a typical focal-conic texture at 366 °C, which is indicative of the SmA phase.

X-ray Diffraction. Discotic liquid crystals based on oxadiazoles are currently under investigation as electron-transport materials for semiconductor applications.[14–16] Materials reported to date, however, are built around a 1,3,5-trisubstituted benzene core terminated with complex substituents, i.e., oxadiazole-based phenylacetylenes with flexible tails (forming nematic mesophases)[14] or tris(oxadiazole) discoids terminated with long alkyloxy tails (forming columnar mesophases).[15] Literature data are available on the electronic structure of P(OP)$_3$,[16] but no data appear to be available on the crystal packing preferences of this molecule. We used single-crystal X-ray structure determinations in order to gain more detailed information about the molecular shape and packing motif of our disk-like P(OP)$_3$ molecule.

Figure 3a shows the ORTEP structure of the P(OP)$_3$ molecule. It is planar, but contrary to our expectations, P(OP)$_3$ does not have C_3 symmetry and is not chiral as

(14) Kim, B. G.; Kim, S.; Park, S. Y. *Tetrahedron Lett.* **2001**, *42*, 2697.
(15) Zhang, Y.-D.; Jespersen, K. G.; Kempe, M.; Kornfield, J. A.; Barlow, S.; Kippelen, B.; Marder, S. R. *Langmuir* **2003**, *19*, 6534.
(16) Sugiyama, K.; Yoshimura, D.; Miyamae, T.; Miyazaki, T.; Ishii, H.; Ouchi, Y.; Seki, K. *J. Appl. Phys.* **1998**, *83*, 4928.
(17) Sheldrick, G. M. *SHELX-97*; Universitat Göttingen: Göttingen, Germany, 1997.
(18) Rossa, L.; Vögtle, F. *Liebigs. Ann. Chem.* **1981**, *3*, 459.

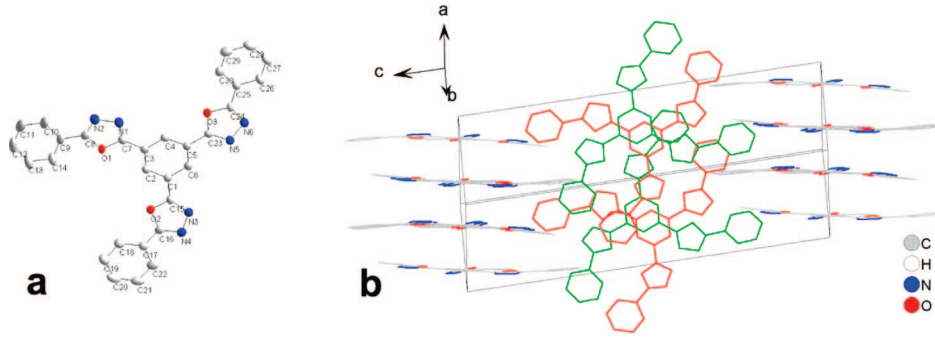

Figure 3. (left) ORTEP structure derived from X-ray analysis; (right) molecular packing motif of P(**O**P)$_3$.

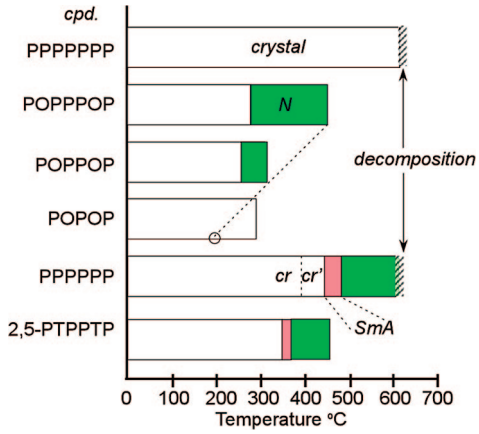

Figure 4. Transition maps showing the phase behavior of several all-aromatic liquid crystals derived from *p*-phenylene parent analogs by substituting 2,5-substituted oxadiazoles or thiophenes for the penultimate rings.

depicted in the structural drawing in Table 4. One of its "arms" is rotated 180° about the C—C bond connecting the central ring to the heterocycle. Figure 3b shows the single-crystal packing motif, an achiral space group, $P\,2_1/n$. There is no apparent long-range packing that might be identified with a precursor to a columnar mesophase. In fact, nearly coplanar molecules stack pairwise in columns with the molecular planes in different columns nearly orthogonal to one another. It is not clear if intermolecular electrostatic dipolar interactions are responsible for the absence of the C_3 symmetry. But we note the antiparallel dipole moments between the "odd" arms of nearest neighbor P(**O**P)$_3$ molecules within a column.

Discussion

We have explored a variety of nonlinear, all-aromatic, thermotropic liquid crystals based on the selective placement of substituted thiophenes and oxadiazoles into *p*-polyphenylene parent molecules. As anticipated from our earlier work with *p*-quinquephenyl derivatives (Figure 1), introduction of nonlinear heterocycles into the higher *p*-phenylenes dramatically depresses transition temperatures and thereby gives access to broad mesophases (Figure 4). Replacing the penultimate phenyl rings in *p*-septiphenyl to get the kinked architecture of *p*-**O**PPP**O**P transforms that intractable solid into a very high temperature nematogen with a broad nematic range (274−444 °C). For the smaller homologue *p*-sexiphenyl with its penultimate rings replaced by 2,5-substituted thiophenes, we found that both the nematic and smectic phases observed in *p*-sexiphenyl are translated to more tractable temperature ranges in P**T**PP**T**P; the smectic phase is lost for the smaller exocyclic bond angles in P**O**PP**O**P, but an even lower temperature nematic survives (Figure 4). It appears that although the polarizability (conjugated aromaticity) and polarity (dipole moments) change on going from thiophene to oxadiazole, molecular geometry is the dominant factor: decreasing the exocyclic bond angle in thiophene ($\epsilon = 148°$) to oxadiazole ($\epsilon = 134°$) lowers transition temperatures and attenuates the mesophase ranges. But the proper geometry without the requisite polarizability suppresses mesophase formation altogether. The intermediate exocyclic bond angle in 2,4-P**T**PP**T**P ($\epsilon = 136°$) is not sufficient to enable liquid crystal formation. Rather, the interrupted electronic conjugation for the 2,4-substitution pattern has a deleterious influence on extended conjugation and decreases the (anisotropic) molecular polarizability of this molecule. The loss of anisotropic electrostatic intermolecular interactions is undoubtedly the reason for the loss of liquid crystallinity in this otherwise modestly nonlinear, six-ring molecule.

Shape changes at the central ring in this class of materials are much more dramatic. The extreme nonlinearity of *m*-P**O**PPP**O**P and *o*-P**O**PPP**O**P (and *m*-P**O**P**O**P) precluded mesomorphism; *m*-P**O**PPP**O**P and *m*-P**O**P**O**P exhibited only crystal-to-crystal transitions before melting directly into the isotropic phase (Tables 2 and 4). The more extreme shape of *o*-P**O**PPP**O**P gives rise to a glassy solid with a glass-transition temperature of 83 °C, i.e., the solid state of this isomer appears to be dominated by geometry-dictated disordered packing which can not be disentangled by annealing below T_g.

Within the para-substituted series, *p*-P**O**PPP**O**P, *p*-P**O**P-P**O**P, and *p*-P**O**P**O**P, one anticipates an increase in crystal lattice energy as the density of oxadiazoles and its associated large electrostatic dipole moment increases. But curiously, the fusion temperatures are relatively constant (Figure 4). And within this series the nematic range decreases dramatically with the removal of phenylene units from the central core, from $\Delta N = 170°$ for *p*-P**O**PPP**O**P to $\Delta N = 43°$ for *p*-P**O**PP**O**P; $\Delta N = 0°$ for *p*-P**O**P**O**P. The absence altogether of a mesophase in *p*-P**O**P**O**P is not surprising, as its fusion temperature is above the estimated hypothetical clearing

temperature (circle in Figure 4). Also the molecular shape (the "aspect ratio") of this five-ring, nonlinear molecule is rather low.

P(**O**P)$_3$ is a special case. In principle, the planar depictions of this molecule with C_3 symmetry (see Table 4) should have sufficient shape anisotropy to exhibit a mesophase. But the X-ray structure shows that the symmetry in the solid state is not C_3. Additionally, the meta linkage interrupts conjugation curtailing the anisotropy of the polarizability. As a result the disk-like P(**O**P)$_3$ molecule in very pure form is not a liquid crystal; a mesophase is briefly observed ($\Delta N \approx 1°$) on cooling if impurities (>1 wt %) are present. Similar observations were found for terminally substituted P(**O**P)$_3$ derivatives having "arms" terminated with *p*-methoxy or -octyloxy tails.[19] Apart from P(**O**P)$_3$'s lack of mesomorphism, the high density of the hole-transport moieties[20] in this trimer may be of interest for applications in organic electronic materials.

In summary, the delicate balance of excluded volume and electrostatic interactions underlying mesophase formation is amplified in this class of all-aromatic mesogen molecules. Generally, we found a depression of transition temperatures as the nonlinearity of the molecular architecture increased. Lastly, accessible mesophases and the extended electronic conjugation in this class of mesogens may enable these otherwise intractable, all-aromatic materials to be candidates for demanding applications requiring highly anisotropic refractive index materials.

Experimental Details

General. Tetrahydrofuran (THF) and diethyl ether were dried over and distilled from sodium/benzophenone prior to use. Reagents were purchased from commercial sources and were used without further purification. The structures of intermediates were confirmed by ^{1}H NMR (Bruker WM250, 250 MHz) and ^{13}C NMR (Varian Gemini 2000−300, 75.46 MHz). Infrared spectra were obtained with a Biorad FTS-7 spectrometer. Transition temperatures were determined by using a PerkinElmer Sapphire differential scanning calorimeter, calibrated with indium (99.99%) (m.p., 156.5 °C, ΔH = 28.315 J/g) and tin (99.99%) (m.p., 232.0 °C, ΔH = 54.824 J/g). The second heating (10 °C min^{-1}) as well as the cooling scan (10 °C min^{-1}) was recorded. To prevent the LCs from subliming out of the sample pans, we used high-pressure DSC sample capsules (Seiko, AL 15). Mesophases were identified with a Nikon Microphot-FX polarizing microscope equipped with a linkam hotstage.

All products were analyzed at the Delft ChemTech mass spectroscopy facility, using with a VG 70 SE mass spectrometer. The accelerating voltage was 70 keV and M+ represents the molecular ion. Additionally, we used a TGA-MS (Netzsch TGA-MS unit STA 409 QMS Skimmer) in order to confirm the purity of our compounds. These experiments were routinely carried out by heating the samples from room temperature to 600 °C under high vac (~10^{-5} Torr). All of the target compounds were highly volatile and the only volatiles detected agree with the molecular ion of the target compound(s) and no other products could be observed. The mass spectrometer was equipped with a TGA balance and in all cases the samples evaporated far below their melting points, and at the end of each experiment, no residual mass (impurities or decomposed product) could be detected.

X-ray Diffraction. Single-crystal data for P(OP)$_3$ were collected on a Siemens SMART CCD diffractometer using graphite-monochromatic Mo Kα radiation (λ = 0.71073 Å) at 173 K. Direct methods revealed all of the non-hydrogen atoms for P(OP)$_3$. All non-hydrogen atoms were refined anisotropically, and the final least-squares refinement converged. Structure solution and refinement were performed with SHELX-97.[17] Crystal data: monoclinic, space group $P2_1/n$, a = 7.5018(7) Å, b = 12.1160(12) Å, c = 26.764(2) Å, β = 97.467(2)°, U = 2412.0(4) Å^3, Z = 48, D_c = 0.351 mg m^{-3}. Data/restraints/parameters: 5046/0/425, R1($I > 2\sigma(I)$) = 0.0515, wR2 = 0.1223, R1(all data) = 0.0901, wR2(all data) = 0.1384.

Synthesis of Model Compounds. *p-POPOP (n = 1).* A 200 mL, one-necked flask was charged with benzoic hydrazide (6.81 g, 50,0 mmol), sodium bicarbonate (4.20 g, 50.0 mmol), and 80 mL of water. The solution was vigorously stirred and a solution of terephthaloyl chloride (5.08 g, 25.0 mmol) in 60 mL THF was slowly added. This reaction mixture was stirred for 6 h and quenched in water. The white solids were collected by filtration and dried under vacuum at 80 °C. Yield: 8.45 g (84%); ^{1}H NMR (300 MHz, DMSO-d_6) δ 7.5−7.65 (m, 6H), 7.95 (d, J = 8.4 Hz, 4H), 8.05 (s, 4H), 10.6 (s, 2H), 10.75 (s, 2H); TLC silica gel (CH_2Cl_2/1,4-dioxane, 90/10); one spot, t_r = 0.1.

A 150 mL, two-necked flask equipped with reflux condenser, magnetic stir bar, and nitrogen inlet was charged with the dihydrazide intermediate (2.0 g, 3.5 mmol), 40 mL of freshly distilled $POCl_3$, and 40 mL of dry toluene. This mixture was heated to reflux for 12 h. The reaction mixture was cooled to room temperature and quenched in ice. The crude off-white product was collected by filtration and dried under a vacuum at 80 °C. Pure *p*-**O**P**O**P was obtained after recrystallization from DMF as colorless crystals. TLC silica gel (CH_2Cl_2/1,4-dioxane, 90/10); one spot, t_r = 0.88; MS (*m*/*z*); 366 (M+), 249, 165, 105, 77, 57. Elemental anal. for *p*-**O**P**O**P. Calcd: C, 72.12; H, 3.85; N, 15.29. Found: C, 71.08; H, 3.81; N, 15.35.

p-POPPOP (n = 2). A 200 mL, one-necked flask was charged with benzoic hydrazide (6.81 g, 50.0 mmol), sodium bicarbonate (4.20 g, 50.0 mmol), and 80 mL of water. The solution was vigorously stirred and a solution of 4,4′-biphenyldicarbonyl dichloride (6.98 g, 25.0 mmol) in 80 mL of THF was slowly added. This reaction mixture was stirred for 6 h and quenched in water. The white solids were collected by filtration and dried under a vacuum at 80 °C. Yield: 8.45 g (85%); ^{1}H NMR (300 MHz, DMSO-d_6) δ 7.5−7.7 (m, 6H), 7.95 (d, J = 8.4 Hz, 4H), 8.05 (d, J = 8.4 Hz, 4H), 10.6 (s, 2H), 10.7 (s, 2H); TLC silica gel (CH_2Cl_2/1,4-dioxane, 90/10), one spot, t_r = 0.1.

A 150 mL, two-necked flask equipped with reflux condenser, magnetic stir bar, and nitrogen inlet was charged with the dihydrazide intermediate (4.0 g, 8.4 mmol), 40 mL of freshly distilled $POCl_3$, and 80 mL of dry toluene. This mixture was heated to reflux for 12 h. The reaction mixture was cooled to room temperature and quenched in ice. The crude off-white product was collected by filtration and dried under a vacuum at 80 °C. A small amount of *p*-**O**PP**O**P was dissolved in CH_2Cl_2/1,4-dioxane (90/10) and chromatographed over a silica gel column. Upon removal of the solvent, small colorless crystals were obtained. TLC silica gel (CH_2Cl_2/1,4-dioxane, 90/10); one spot, t_r = 0.8; ^{1}H NMR (300 MHz, $CDCl_3$) δ 7.52−7.61 (tt, 2H), 7.85 (d, J = 8.6 Hz, 4H), 8.16−8.21 (m, 4H), 8.28 (d, J = 8.6 Hz, 4H); MS (*m*/*z*); 442 (M+), 325, 169, 105, 77. Elemental anal. Calcd for *p*-**O**PP**O**P: (%) C, 76.01; H, 4.10; N, 12.66. Found: C, 76.10; H, 4.00; N, 12.59.

(19) Choi, E.-J. 2007, private communication.
(20) Zhang, Y.-D.; Jespersen, K. G.; Kempe, M.; Kornfield, J. A.; Barlow, S.; Kippelen, B.; Marder, S. R. *Langmuir* **2003**, *19*, 6534–6536.

p-POPPPOP (n = 3). The synthesis of 2-(4-bromophenyl)-5-phenyl-1,3,4-oxadiazole was reported elsewhere.[6] A 50 mL, two-necked flask equipped with magnetic stir bar, reflux condenser, and argon inlet was charged (under argon atmosphere) with 2-(4-bromophenyl)-5-phenyl-1,3,4-oxadiazole (0.9 g, 3 mmol) and 6 mol % tetrakis-(triphenyl-phosphine)palladium(0) (0.16 g, 0.14 mmol). A volume of 20 mL of dimethoxyethane (DME) was added and the resulting yellow solution was stirred for 10 min at room temperature. 1,4-Phenylenebisboronic acid (0.2 g, 1.2 mmol) and 20 mL of 2 M Na_2CO_3 were added, and this mixture was refluxed under argon atmosphere for 24 h. After cooling to room temperature, the reaction mixture was diluted with 50 mL of water and filtered. The solids were washed with acetone and dichloromethane and dried under a vacuum overnight at 80 °C. Pure *p*-**O**PPP**O**P (0.35 g, 56%) was obtained as colorless platelets after two recrystallizations from chlorobenzene. MS (*m*/*z*): 366 (M+), 249, 222, 165, 105, 83. Elemental anal. Calcd for *p*-**O**PPP**O**P: C, 78.75; H, 4.28; N, 10.80. Found: C, 78.25; H, 4.23; N, 10.72.

Synthesis of 2,5-PTPPPTP and 2,4-PTPPPTP. The synthesis of 2-phenyl-5-thiopheneboronic acid and 4-phenyl-2-thiopheneboronic acid was reported elsewhere.[6]

2,5-PTPPTP. A 50 mL, two-neck flask equipped with magnetic stir bar, reflux condenser, and argon inlet was charged (under an argon atmosphere) with 4,4′-dibromobiphenyl (0.094 g, 0.30 mmol) and tetrakis(triphenylphosphine)palladium(0) (0.040 g, 0.035 mmol). A volume of 5 mL of dimethoxyethane (DME) was added and this yellow solution was stirred for 10 min at room temperature. 2-Phenyl-5-thiopheneboronic acid (0.16 g, 0.80 mmol) and 5 mL of 2 M Na_2CO_3 were added, and this mixture was refluxed under an argon atmosphere for 24 h. After cooling to room temperature, the reaction mixture was diluted with 50 mL of water and filtered. The solids were washed with acetone and dichloromethane and dried under a vacuum overnight at 80 °C. Pure 2,5-P**T**PP**T**P (0.11 g, 79%) was obtained as yellow platelets after two recrystallizations from 1,2,4-trichlorobenzene. MS (*m*/*z*): 470 (M+), 388, 235, 169, 69, 55. Elemental anal. Calcd for 2,5-P**T**PP**T**P: C, 81.66; H, 4.71; S, 13.63. Found: C, 81.60; H, 4.73; S, 13.45.

2,4-PTPPTP. Similar procedure as described for 2,5-P**T**PP**T**P. Pure 2,4-P**T**PP**T**P (0.10 g, 71%) was obtained as yellow platelets after two recrystallizations from 1,2,4-trichlorobenzene. MS (*m*/*z*): 470 (M+), 235, 169, 98, 73, 60. Elemental anal. Calcd for 2,5-P**t**PP**t**P: C, 81.66; H, 4.71; S, 13.63. Found: C, 81.66; H, 4.70; S, 13.35.

Synthesis of *m*-POPOP. *m*-P**O**P**O**P was made in a similar fashion as described for *p*-P**O**P**O**P, starting from isophthaloyl chloride. TLC silica gel (CH_2Cl_2/1,4-dioxane, 90/10); one spot, t_r = 0.95. MS (*m*/*z*): 518 (M+), 401, 105. Elemental anal. Calcd for *m*-P**O**P**O**P: C, 72.12; H, 3.85; N, 15.29. Found: C, 69.66; H, 3.90; N, 14.44.

Synthesis of *o*-POPPPOP. *Synthesis of 4,4″*-o-*Terphenydicarboxylic Acid.* A 200 mL, one-necked flask equipped with Claisen adapter and argon inlet was charged with 70 mL of carbon disulfide, *o*-terphenyl (7.6 g, 0.033 mmol), and oxalyl chloride (25 g, 0.197mol). This solution was cooled to 0 °C and anhydrous aluminum chloride (10 g, 0.75 mol) was added in several batches. The dark-brown mixture was stirred for 1 h at 0 °C, after which an additional batch aluminum chloride (10 g, 0.75 mol) was added. The ice bath was removed, and stirring was continued overnight at room temperature. The reaction mixture was slowly quenched into a mixture of dilute hydrochloric acid and crushed ice. The carbon disulfide was evaporated under reduced pressure and a pale yellow product was filtered and washed with dilute hydrochloric acid and water. The crude product was treated with a 10% KOH solution in methanol. The obtained potassium carboxylate was acidified using concentrated HCl and the filtered product was washed with water, recrystallized from a mixture of ethanol and water (7:1 v/v), and dried under a vacuum at 60 °C: T_m = 345 °C (dec) (Lit.:[18] 317−320 °C); ^{1}H NMR (400 MHz, DMSO-d_6) δ 12.94 (s, 2H), 7.81 (d, J = 8.2 Hz, 4H), 7.51 (m, J = 31.2 Hz, 4H), 7.23 (d, J = 8.2 Hz, 4H).

Bis(benzoylhydrazide) 4′,4″-o-*terphenydicarboxylic Acid.* Benzoic hydrazide (0.855 g, 6.28 mmol) was dissolved in a mixture (20 mL) of methylene chloride and pyridine (1:1 v/v). To this solution was added 4,4″-*o*-terphenyldicarbonyl dichloride (1.12 g, 3.14 mmol) in 20 mL of methylene chloride. The reaction mixture was stirred at room temperature under a dry argon atmosphere, and after about 30 min, the reaction mixture was heated at 90 °C overnight. The reaction mixture was concentrated to about 10 mL by evaporating the solvent under reduced pressure. The residue was cooled to room temperature and poured into 250 mL of water. The resulting precipitate was collected by filtration, thoroughly washed with water, and dried under a vacuum at 60 °C.

Bis(5-phenyl-1,3,4-oxadiazole-2-diyl) 4,4″-o-*terphenyl.* To a solution of phosphoryl chloride (10 mL) and acetonitrile (30 mL) the dihydrazide intermediate (0.500 g, 0.902 mmol) was added. The reaction mixture was heated at 110 °C overnight and then concentrated to about 20 mL by evaporating the solvent under reduced pressure. The residue was cooled to room temperature and carefully quenched in 200 mL of ice−water to hydrolyze the residual $POCl_3$. The resulting solid was washed with water, collected by filtration, dried under a vacuum at 60 °C, and purified using column chromatography—silica gel with an eluent of hexane and ethyl acetate (1:1 v/v). Crude product was further purified by reprecipitation: dissolved in chloroform, filtered by a PTFE membrane filter, crystallized from hexane, and dried under a vacuum at 60 °C. TLC (silica gel, hexane/ethyl acetate = 1:1, v/v), R_f 0.84; ^{1}H NMR (400 MHz, $CDCl_3$) δ 8.11 (d, J = 7.9 Hz, 4H), 8.03 (d, J = 8.5 Hz, 4H), 7.52 (s, 4H), 7.51 (m, J = 40.7 Hz, 6H), 7.34 (d, J = 8.5 Hz, 4H). MS (*m*/*z*): 518 (M+), 401, 331, 315, 282. Elemental anal. Calcd for *o*-P**O**PPP**O**P: C, 78.75; H, 4.28; N, 10.80. Found: C, 77.66; H, 4.45; N, 10.56.

Synthesis of *m*-POPPPOP. *m*-P**O**PPP**O**P was synthesized via a similar route as described for *o*-POPPPOP, starting from *m*-terphenyl. ^{1}H NMR (300 MHz, DMSO-d_6 at 120 °C) δ 8.25 (d, J = 8.4, 4H), 8.15 (m, 4H), 8.09 (s, 1H), 8.03 (d, J = 8.4, 4H), 7.82 (dd, J = 7.5, 2H), 7.65 (m, 7H). MS (*m*/*z*); 518 (M+), 418, 399, 207, 105. Elemental anal. Calcd for *m*-P**O**PPP**O**P: C, 78.75; H, 4.28; N, 10.80. Found: C, 78.05; H, 4.37; N, 10.58.

Synthesis of P(OP)$_3$. A 500 mL, one-necked flask was charged with benzoic hydrazide (4.09 g, 30 mmol) and 30 mL of anhydrous THF. The solution was cooled to 0 °C and a solution of 1,3,5-benzenetricarbonyl trichloride (2.65 g, 10 mmol) in 20 mL of dry THF was slowly added, followed by 5 mL of dry pyridine. The reaction mixture was stirred for 12 h and allowed to warm to room temperature. The reaction mixture was quenched in water and the white solids were collected by filtration and dried under a vacuum at 60 °C. The hydrazide intermediate was recrystallized from hot DMSO and afforded colorless crystals. Yield: 3.65 g (65%). ^{1}H NMR(300 MHz, DMSO-d_6): δ 7.5−7.7 (m, 9H), 7.95 (d, J = 8.4 Hz, 6H), 8.66 (s, 3H), 10.5−11.0 (b, 6H). TLC silica gel (CH_2Cl_2/1,4-dioxane, 90/10): one spot, t_r = 0.1.

A 100 mL, two-necked flask equipped with reflux condenser, magnetic stir bar, and nitrogen inlet was charged with the hydrazide intermediate (2.0 g, 3.5 mmol) and 30 mL of freshly distilled $POCl_3$. This mixture was heated to 70 °C for 24 h. The reaction mixture was cooled to room temperature and quenched in ice. The crude off-white product was collected by filtration and dried under vacuum

at 80 °C. The crude $P(OP)_3$ was dissolved in CH_2Cl_2/1,4-dioxane (90/10) and chromatographed over a silica gel column. Upon removal of the solvent small colorless crystals were obtained. TLC silica gel (CH_2Cl_2/1,4-dioxane, 90/10): one spot, $t_r = 0.85$. MS (*m*/*z*): 510 (M+), 393, 105. ^{1}H NMR (400 MHz, DMSO-d_6) δ 9.0 (s, 3H), 8.26 (d, $J = 8.0$, 6H), 7.5−7.7 (m, 9H), 7.95 (d, $J = 8.4$ Hz, 6H), 8.66 (s, 3H), 10.5−11.0 (b, 6H). ^{13}C NMR(75 MHz, DMSO-d_6 at 116 °C): δ 164.4, 162.3, 131.5, 128.7, 126.6, 126.5, 125.6, 122.7. Elemental anal. Calcd for P(**O**P)$_3$: C, 70.58; H, 3.55; N, 16.46. Found: C, 70.44; H, 3.61; N, 16.41.

Acknowledgment. This work was supported by NSF Grants DMR-9971143 and DMR-0605923 and in part by KOSEF Grant R01-2001-00433.

Supporting Information Available: Complete crystallographic information for P(**O**P)$_3$ (CIF file), including atomic coordinates for all atoms, bond lengths and angles, anisotropic displacement parameters, and torsion angles. This material is available free of charge via the Internet at http://pubs.acs.org.

CM701862W